AN ABSTRACT OF THE THESIS OF

Mee-ya A. Monnin for the degree of Honors Baccalaureate of Science in Fisheries and Wildlife Sciences presented on July 10, 2014. Title: Weight watching: Morphometric indices of ontogenetic and reproductive stages in Weddell seals

Abstract approved: _____
Markus Horning

We investigated ontogenetic changes in body morphology of Weddell seals (*Leptonychotes weddellii*) using three three-dimensional (3D) photogrammetry, to estimate surface areas and body volumes for 42 Weddell seals. We sampled ten weaned pups, twelve juveniles (age one or two years), 11 non-breeding adult females, and 9 adult females who had recently weaned a pup. We developed predictive values for surface-area-to-volume (SA:V) ratios of juvenile seals using a morphological growth projection based on data from pups and adult females, then compared to measured values.

Juveniles were longer than pups but groups overlapped at their extremes. Juveniles had significantly smaller SA:V ratios than pups. However, the shortest juveniles had larger SA:V ratios than the longest pups. Within both groups, SA:V ratios declined with increasing body length. Juveniles and post-reproductive female SA:V ratios consistently exceeded values predicted from the pup-to-adult growth projection, suggesting that morphological changes as well as increasing body length influenced SA:V ratios in juveniles. Ultrasonically measured blubber thickness indices were lower in juveniles and post-reproductive females, but mean body densities estimated from mass and volume did not differ. We suggest that surface area, volume, and blubber morphometrics may provide meaningful indicators of body condition not identified with ratios of adipose to lean tissue.

Key Words: photogrammetry, morphometrics, surface area, body volume, Weddell seal, thermoregulation, *Leptonychotes weddellii*, body condition, body density

Corresponding e-mail address: m.a.monnin@gmail.com

Weight watching: Morphometric indices of ontogenetic and reproductive stages in Weddell seals

by

Mee-ya A. Monnin

A PROJECT

submitted to

Oregon State University

University Honors College

in partial fulfillment of
the requirements for the
degree of

Honors Baccalaureate of Science in Fisheries in Wildlife Sciences (Honors Scholar)

Presented July 10, 2014
Commencement June 2015

Honors Baccalaureate of Science in Fisheries and Wildlife Sciences project of Mee-ya A. Monnin presented on July 10, 2014.

APPROVED:

Markus Horning, Mentor, representing Fisheries and Wildlife Sciences

---

Michelle Kappes, Committee Member, representing Fisheries and Wildlife Sciences

---

Chris Langdon, Committee Member, representing Fisheries and Wildlife Sciences

---

Toni Doolen, Dean, University Honors College

I understand that my project will become part of the permanent collection of Oregon State University, University Honors College. My signature below authorized release of my project to any reader upon request.

Mee-ya A. Monnin, Author

ACKNOWLEDGEMENT

I would like to express my utmost gratitude and appreciation of many individuals and institutions that have contributed to my education and research at Oregon State University while I pursed my honors bachelor degree. First and foremost, I would like to thank the man who has acted as my boss, thesis advisor, and mentor for the last 3 years, Dr. Markus Horning. Without Markus, none of the major accomplishments of my undergraduate degree would be a reality. His guidance and support has been instrumental towards my growth and development as a budding scientist. I would also like to thank my committee members, Dr. Michelle Kappes and Dr. Chris Langdon, for their willingness to help and their flexibility as I finished this endeavor. However, especially to Dr. Kappes, whose advice and encouragement was indispensable as I finished up my final draft of this thesis.

Funding for this project was provided by the National Science Foundation. Additionally, I would like to thank all the amazing individuals who help run support all of the fantastic research that comes out of McMurdo Station, Antarctica. Their logistical and technical support made this project possible. A special thanks to Dr. Jo-Ann Mellish and Dr. Allyson Hindle, two of three fantastic P.I.s that fashioned the 'triad'. Additionally, to the remaining members of my field team B470, John Skinner and Dr. Rachel Berngartt, your patience, support, and provision of laughter has been unforgettable. To the support staff at Photomodeler and Rhino, for spending literally hours answering all of my obscure questions about their programs, as I attempted to create my first model Weddell seal, without your help I would likely still be sitting in

front of my computer. To all of the folks at the Marine Mammal Institute and Hatfield Marine Science Center, for their support and encouragement. I feel privileged and proud to state that I have worked alongside the amazing people and scientists who work at Hatfield Marine Science Center and specifically within the Marine Mammal Institute.

Lastly, I would like to express my gratefulness for my personal support system, whose love and support has helped me stay strong and grow throughout the last 6 years. I thank my parents, Mike and Gracie Monnin, for their undying encouragement and support as I have gone through one (often unnerving) adventure to the next; to the woman who is my rock, my role model, and my other half, Aunt Clare; to the best friend there ever was Rachel Miller; to the unbelievable and unending support (not to mention provider of many home cooked meals) of LeeAnn Baker; to my sisters of light, love, and dancing, who never fail to make me smile, Sunny Oveson and Kat Perez; to the many years of love provided my Sarah Charles; to Susan and Francis Reedy, whose love and support over the last year and half has truly changed my life for the better; and finally to my partner in crime, adventure, life, and love, Daniel Reedy.

TABLE OF CONTENTS

LIST OF FIGURES

Figure Page

LIST OF TABLES

Table Page

Weight watching: Morphometric indices of ontogenetic and reproductive stages in Weddell seals

INTRODUCTION

The total amount of heat loss an animal experiences is proportional to the surface area (SA) of that animal (Innes et al. 1990). Marine mammals are exposed to both water and air, two environments of highly distinct thermal characteristics (Hokkanen 1990; Berta et al. 2005; Learmonth et al. 2006). The thermal conductivity of water is 25 times greater than that of air, and aquatic homeotherms may experience a 1.5-4.5 greater rate of heat loss in water than air (Nadel 1984). Due to the high thermal conductivity and high specific heat capacity of water, the thermal environment of marine mammals (especially those located in the polar/sub-polar regions) are those with the highest cooling potential encountered by mammals (Irving 1973). Hence the reason as to why thermoregulation is a vital biological factor for homeotherm organisms existing in polar and sub-polar latitudes. With total heat loss being proportional to the SA of an animal, it is unsurprising that marine mammals typically have a smaller surface-area-to-volume-ratio (SA:V) than terrestrial animals of comparable size or body mass (Bryden 1972; Ridgway 1972; Iversen and Krog 1973).

Larger objects generally have a smaller SA:V ratio, thereby generally making it energetically advantageous to be larger (Schmidt-Nielsen 1984). Typically it is assumed that younger and smaller individuals have a higher SA:V ratio and are therefore more energetically challenged than their older, and presumably larger, counterparts (Blix and Steen 1979; Innes et al. 1990). Young and/or lean animals may be at risk of elevated heat loss (Innes et al. 1990; Watts et al. 1993; Hansen and Lavigne 1997; Roscow 2001; Noren et al. 2008); however, a well-developed blubber layer, in addition to large body size, helps mediate this heat loss.

Weddell seals (*Leptonychotes weddellii*) are the southernmost breeding mammal (Dearborn 1965) and are well studied in McMurdo Sound. Their distribution is circumpolar, however they are best associated with the fast ice of Antarctica where they are found hauled out for considerable portions of the day during their breeding season, austral spring. This study was conducted in Erebus Bay, McMurdo Sound, Antarctica (77.7˚S, 166.5˚E), where air temperatures can drop below -30˚C in the early summer, but may rise above freezing during mid- and late summer. McMurdo Sound water temperatures are consistently near -1.9˚C.

The mean age at first reproduction of Weddell seals in the Erebus Bay area is 7.6 years of age (Hadley et al. 2006), with females typically producing one pup every 1.5 – 2.2 years thereafter (Stauffer et al. 2013). Pre-parous females that have not yet reproduced, are termed “prebreeders”, while females who may skip having a pup some years after primiparity are termed “skipbreeders” (Stauffer et al. 2013). Parous, adult females typically have a single pup during the pupping season of September through November and nurse their pups in fast ice colonies (Kaufman et al. 1975; Elsner et al.

1977; Kooyman and Kooyman 1981; Stauffer et al. 2013). As capital breeders, the mothers cease lactation and the pups are weaned at 5 – 6 weeks (Stauffer et al. 2013).

Like most phocid pups, Weddell seal pups are extremely rotund after nursing for 5-6 weeks, leaving their fasting mother noticeably emaciated. Over the course of the next 1-2 years, young seals undergo substantial developmental changes (Burns and Testa 1997; Burns 1999), even though juveniles retain a similar mass as pups. Juveniles grow in length, shrinking in girth, and often appear visually leaner than pups (Kooyman 1968).

Adult females in this study were available in two subgroups of differing body conditions: non-reproductive females (NRF) in good body condition that were not pregnant in the sampling year, and post-reproductive females (PRF) that had just weaned their pup and were therefore in comparably lean condition at the end of the lactation period.

We speculate that contrary to classic assumptions, juveniles may have a less advantageous (larger) SA:V ratio than pups. Typically SA estimates for marine mammals are obtained by direct measurements or through geometric approximations (Innes et al. 1990). Here, we used Photomodeler version 6.0 (EOS Systems Inc., Vancouver, Canada), a three-dimensional (3D) modeling program, to investigate whether juveniles have slimmer, more unfavorable body conditions, and if so, whether there is a pronounced effect. NRFs (7+ years) and pups were used to develop predicted values for SA and volume (V) for juveniles via a morphometric growth projection based on data from pups and adult females, then compared to measured values.

The specific objectives of this study were to: 1) quantify and compare approximate SA and V values of Weddell seals created via a 3D modeling program; and 2) determine whether 3D photogrammetry may be an appropriate determinant of body condition in Weddell seals. I predicted that contrary to class assumptions, juveniles have a larger, and therefore less advantageous, SA:V than pups. Additionally, I predicated that 3D photogrammetry provides a more complete and accurate approximation of body condition than most currently utilized techniques.

METHODS

Study Animals

We collected photos from 42 animals (F = 30, M = 12) from four experimental groups: pups (weaned), juveniles (age 1 – 2 years), non-reproductive females (NRF; non-breeding adult females ie. prebreeders and skipbreeders), and post-reproductive females (PRF; females who have recently weaned their pups). We sampled in 2011 (n=14) and 2012 (n = 28), for a total of 10 pups, 12 juveniles, 11 NRFs, and 9 PRFs.

An addition pup (female) from 2011 was excluded from all reported findings, as animal LW11-15 was the only animal in its group to be sampled in 2011. Additionally, LW11-15 was not used for any other project parts, such as telemetry. Therefore, a total of 43 animals were handled from 2011 to 2012 (F = 31, M = 12), although only 42 were used in this study.

Field Procedure

All animal work on Weddell seals was conducted between October 25 and December 14 of 2011 and 2012, in McMurdo Sound (Ross Sea region, Antarctica), under ACA permit #2011-003, NMFS permit #15748 and all applicable institutional animal care permits.

Photogrammetry is the science of making measurements from photographs (Baker 1960). 3D photogrammetry uses multiple images from various perspectives to obtain spatial information and can be used for the measurement of morphometric variables via a 3D virtual recreation of the subject (Waite et al. 2007).

We used 3D photogrammetry to create spatially referenced 3D computer wire-frame models of individual seals from four time-synchronous digital still images (Waite et al. 2007). These models were then used to estimate SAs and volumes of individual animals. Individual seals were chemically sedated using intramuscular injections for induction and intravenous injections for maintenance (Mellish et al. 2010). Sedation was required for other aspects of the project unrelated to photogrammetry, including attachment of telemetry devices. Following sedation, animals were weighed to the nearest 0.5 kg in a tarpaulin suspended under a digital scale from a large tripod (Mellish et al. 2010). Thickness of subcutaneous layer (blubber thickness) was measured in ten locations via a handheld ultrasound (Mellish et al. 2004; Mellish et al. 2007; Mellish et al. 2011).

The photogrammetry procedure was improved between the first and second field season. Throughout 2011, photogrammetry was completed after the induction of sedation had taken effect and before other procedures were initiated. The animals were not heavily sedated and therefore often fairly active, reacting to any gust of wind, movement, or sound. Many photos from the first season showed the seals in curved or twisted positions, making it more difficult to create accurate models. In 2012, photogrammetry was performed at the *end* of all other procedures, thereby allowing the animal to remain fully sedated. The animals were thus less prone to move and could be positioned into the straightest alignment possible. The seals could also be moved onto fairly flat terrain to increase the accuracy of the ground plane on the models.

We used marked ropes to assist with point matching identification. Eight marked ropes were placed on the body of the sedated seals: the tallest point on the head (A), the dip of the neck (B), the base of the tail (C), the axial girth directly behind the front flippers (E), halfway between E and C (Rope F), halfway between E and F (rope D), halfway between F and C (rope G), and halfway between G and C (rope H) (Figure 1). The ropes were thus placed throughout the animal's body, effectively segmenting the body. For modeling purposes, we paid particular attention to place ropes at the highest and lowest points of the animal in relation to the ground. We furthermore added a section of tape with marked points along the center of the seal's face from top of the head to the tip of the nose, allowing for more accurate modeling of the head (Figure 1). Four large aluminum measuring sticks were placed around the seal and were used for scaling. For contrast and accurate modeling of the ground plane, the seals remained on the black weighing tarpaulin, or were moved back onto it, and the tarpaulin was pulled flat to the

ground, thus preventing artificially raised or depressed points. Two cubes were also placed at the head and foot of the seal to help with the identification of matching photos for sequential sets. The cubes had different lettering on different faces and were rotated between sequential photo sets.

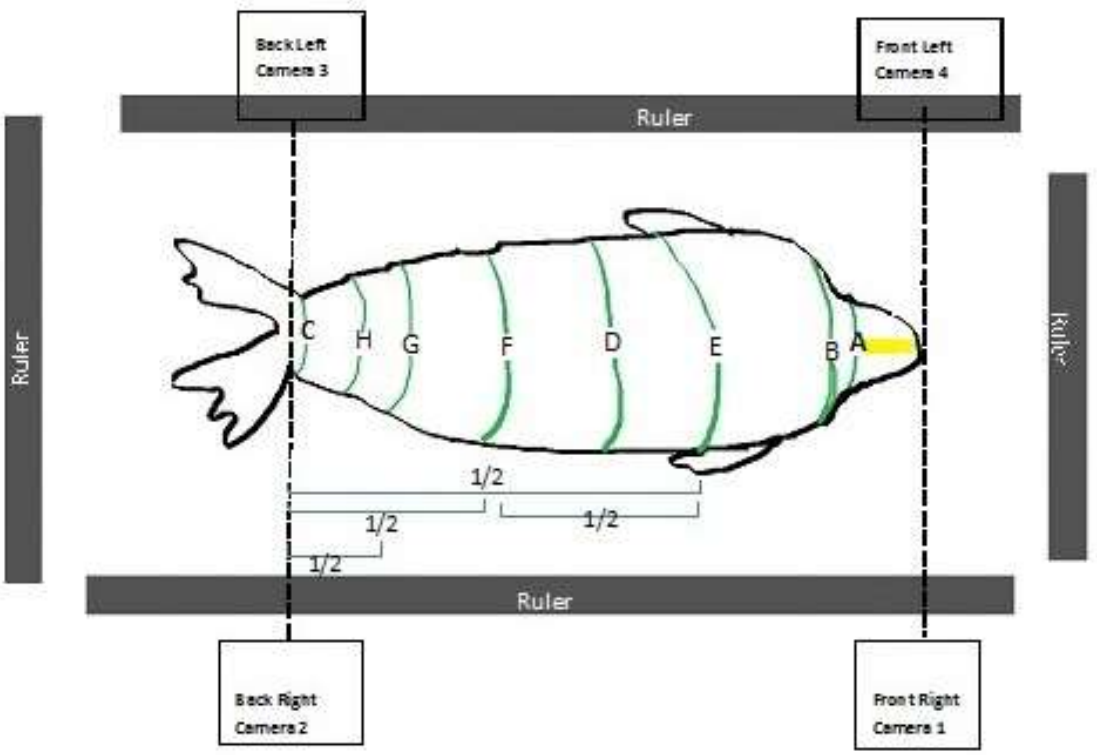

Figure 1. Photogrammetry set up

In 2011 we used four Nikon D100 cameras and in 2012 four Olympus PEN EPL-1 cameras. The Nikon D100's had zoom lenses set to the widest possible angle of 17mm focal length, while the Olympus EPL-1's had 14 mm fixed focal length lenses. To maintain a constant depth of field, images were taken in aperture-priority automatic exposure mode and the aperture of the lenses was set to f/16, and the cameras to ISO 800. Exposure compensation was set to +1.3 to increase the visibility of fur features on

animals. JPEG (.jpg) image files were stored in the highest available resolution and lowest compression. The cameras were calibrated following instructions provided by the 3D modeling software, Photomodeler, by taking multiple photos of a 1m x 1.3m printed calibration grid (black patterns on a white background) whilst ensuring the cameras settings were noted for use in the field.

To collect image sets, 4 individual camera operators assumed positions by one of four corners around the seal with their individually assigned cameras. The cameras were placed to the right and left of the animal, two individuals on either side of the animal at the base of the animal near the first rope (where the flippers meat the girth of the body) and two at the head (Figure 1). The nose and the back rope had to be in the imaging area of all 4 cameras. Perpendicular camera angles are reported best for the highest accuracy of photogrammetric measurements (Photomodeler manual), however it was important that the entire right or left side of the animal was visible in at least two photos for point to point matching. Because of the shape and morphology of a Weddell seal, the animal is widest above the ground plane and narrows slightly at the point at which the animal touches the ground plane, points like these are often difficult, if not impossible, to identify via photos. With the use of ropes, the flattened tarpaulin upon which the subjects rested, and the measuring sticks, it was possible to approximately model the bottom of the animal. All four photos were collected simultaneously, ensuring the animal's position did not change between images and all points in the photos would match. Several sets of photos were taken as a precaution.

Creating the Three-dimensional Models

The photos were first downloaded, cataloged, and then analyzed. The photo sets with the subjectively best (clearest or apparently sharpest) photos were selected and inputted into Photomodeler. The photos were then referenced using features on the four large stainless steel measuring sticks placed around the seal that were recognizable in at least two adjacent images. Referencing is the technical term in Photomodeler by which the software can automatically determine the relative location and orientation of the four cameras with respect to one another (Photomodeler manual). The measuring sticks had marks at distinct distances apart (25 cm) and were carefully marked with different colored tape to ensure the highest probability of identification (due to the harsh lighting conditions and contrast of the photos, this proved helpful). A known distance measurement between multiple reference markers on a measuring stick provides the 3D modeling program with ability to scale the model and accurately approximate measurements from the completed model.

The pair of photos taken from the same side of an animal was typically referenced first and then cross referenced with a photo of the opposite side next. In some instances where referencing proved difficult (i.e. obscured or unrecognizable points) additional features were used for referencing (i.e. the cubes, edges of the tarpaulin, etc.). After referencing and scaling the photos, the model was oriented by selecting “x” and “y” planes. The “x” plane was defined from left to right and the “y” plane as front to back. The “z” plane was therefore defined by the bottom of the animal and the tarpaulin. To

create the model of the seal itself, points using the markers on the ropes laying on the fur of the seal were selected and matched in multiple images. Eight "open semi circles" corresponding to the eight ropes were created after connecting the points on each rope using a "curve through points" tool (hence, the importance of the placement of the ropes). It was important that the last rope on the animal (by the tail) be at the very base of the animal directly before the tail (ensuring more consistent and complete measurements). An additional 9th short arch was created using the points from the tape on the front of the face of the animal. Using those points and the ground plane, an additional semicircle was created before the nose point. All remaining points were connected using "Mark Lines Mode", allowing the creation of triangles and rectangles using straight lines.

Due to the angle of the photo, the positioning of the seal, and raised folds in the tarpaulin, the view of the ground plane may be obscured at the base of certain ropes. In this situation points were created points as close to the ground plane as was visible. These points were then connected to points identifiable as being on the ground plane, thereby creating triangles from the ground plane to the nearest visible points (Figure 2).

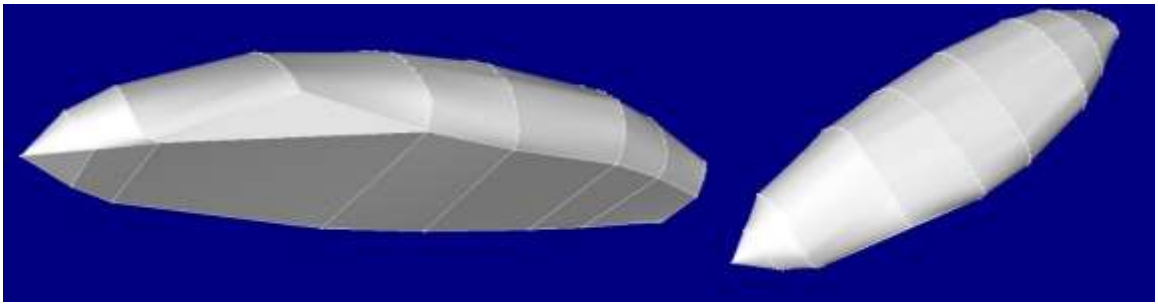

Figure 2. Example of a complete 3D wireframe model with surfaces as visualized in Photomodeler, view of the left side of the animal from below (left) and the left side of the animal from above (right). Note the triangle created to connect the axial girth (rope E) to the ground plane – see text for details.

The ground plane was created by connecting the bottom most points (only those that were identifiable) around the base perimeter of the seal. On the bottom of the seal model (an animal's ventral aspect), the lowest points were connected to the lowest point opposite the body across the ground plane of the animal, creating a line between the points. At the axial girth of the animal, the last point visible on the rope was typically much higher and thus was connected with a line to the lowest points adjacent to the axial girth, creating a triangle on either side of the animal.

After marking all visible points, connecting points via curves or straight lines and creating the ground plane, the "LOFT" surfacing tool was used on the completed wire-frame to surface the model from one semicircle to the next and between all other rectangles and triangles on the model. The entire model was created using the LOFT tool, with the exception of the space between the first semicircle on the head to the nose. The head of the animal was surfaced using the "cone" surfacing tool, connecting the point of the nose to the first semicircle. The SA of this model was then calculated in Photomodeler.

The fully surfaced 3D wire-frame model was exported as a wavefront (.obj) file with all settings (cylinders, curves, surfaces) set to NURBS and then imported into another 3D modeling software, Rhino version 4.0 (Robert McNeel and Associates, Seattle, Washington, U.S.A.), using the "small object (centimeters)" selection (the same scale used in Photomodeler). Although the model in Photomodeler was surfaced,

importing the model into Rhino results in a wireframe model void of surfaces. Rhino is capable of calculating volume and SA measurements from a 3D wireframe.

Importing the model into Rhino resulted in holes in the wireframe that required repair before obtaining measurements from the program. These holes were repaired by first highlighting and selecting the entire model and selecting the following steps in the command tool bar, re-selecting the entire model between giving each command: “Show Edges”, “Explode”, and “Join”. Highlight and selecting the entire model again, and in the main toolbar of Rhino under “Analyze” selecting “Mass Properties” and “Area” for the SA value and “Volume” for the volume measurement.

Modeling the Expected Growth Curve

In order to determine whether juveniles might have a SA:V ratio that is larger than expected, we developed a predicted value for the transitional stage between pups and adult animals based on the assumption of proportional growth. Since the SA of a three-dimensional, generally cylindrical object increases with the square of the radius while volume increases with the cube, a simple linear regression from pups to adult females would not accurately predict the progression of SA:V ratios in relation to body length.

We therefore investigated multiple geometric models for estimating the predicted values for SA and volume of an expected growth curve from pups to NRFs. Traditionally,

several types of geometric models have been used to approximate morphometric thermoregulatory parameters in pinnipeds, such as a half sphere, half cylinder, and bi-conical approximations. We created a more representative model using full cones and truncated cones defined by five girths (A,B,C,E,F) positioned along five standardized sections of the body length (L_1- L_5, expressed in % of body length) (Figure 3; Table 1). The mean values of photogrammetrically determined girths from pup and NRF wireframes for all circumferences shown in Figure 3 were proportionally progressed from pups to NRFs in relation to body length.

The resulting relationship between surface-area-to-volume ratios (SA:V) and body length was best described by a power equation of the type $y = ax^b$ after an adjustment through an additional scaling factor applied to volumes. A power equation was then fit to the calculated photomodeler values through pups and NRF; the resulting equation represents the Expected Growth Curve (EGC). Residuals for the expected growth curve were calculated using the actual pup and NRF data versus the predicted values for those age classes from the EGC. We estimated the mean body density as body mass (kg) / body volume (l).

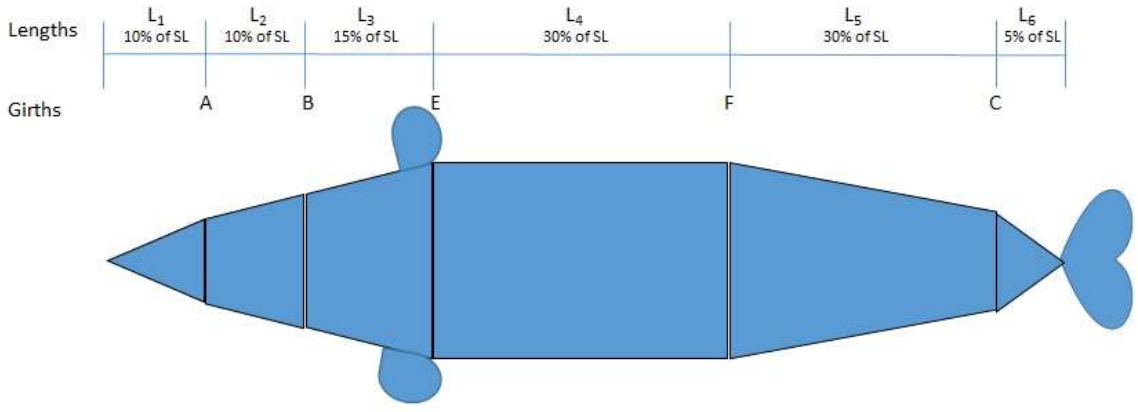

Figure 3. Explanation and location of parameters of the cones and truncated cones model used to create the expected growth curve (EGC).

Table 1. Parameter listing of the cones and truncated cones model used to create the expected growth curve

	SL	L_1	Girth of A G(A)	A's % of SL	Radius of A r(A)	V of section A V(A)	SA of section A SA(A)	V of section A-B V(AB)	SA of section AB SA(AB)	L_2	G(B)	%SL G(B)	R(B)	V (BE)	SA (BE)	L_3	G(E)	%SL G(E)	R(E)	V (EF)	SA (EF)	L_4	G(F)	%SL G(F)	R(F)	V (FC)	SA (FC)	L_5	G(C)	%SL G(C)	R(C)	V (C)	SA (C)	L_5
Extrapolated 5 steps																																		
Known pup values																																		
Synthesized 10 steps																																		
Known NRF values																																		
Extrapolated 5 steps																																		

Statistical Data Analysis

Generalized linear models were used to explore the effect of length and age class on seal body condition (SA:V ratios). The following statistical differences were analyzed using student's two sample, two-tailed t-tests, SA:V ratios for pups and juveniles; mean density between juveniles and pups as well as PRF and NRF; and sum of blubber depths between pups and juveniles in addition to NRF and PRF. All statistical analyses were performed in Excel 2013 (Microsoft Corporation, Redmond, Washington, U.S.A.) and/or Minitab 16 (Minitab Inc., State College, Pennsylvania, U.S.A.) with $\alpha = 0.05$ and degrees of freedom = n – 2.

RESULTS

The SA increased with the volume of individuals, with adult females (n=20) having generally larger values for both parameters than juveniles (n=12) and pups (n=10), respectively (Figure 5). However, juveniles and pups overlapped considerably with respect to both parameters. On average, juveniles were longer than pups, with the shortest juveniles having lengths comparable to the longest pups (Figure 6). The two groups of adult females mostly overlapped in body length (Figure 6) while SA and volumes in NRFs (n=11) tended to be higher than in PRFs (n=9). The smallest (shortest) juveniles appeared to have a larger SA:V ratio than the largest (longest) pups of similar body length. However, on the whole the SA:V ratio of juveniles was lower than that of pups (Figure 4). A student's t-test indicates a possible difference in SA:V ratios for pups versus juveniles (n=22, $t = 2.0$, $P=0.058$). SA:V ratios averaged 0.15 ± 0.009 for pups and 0.14 ± 0.014 for juveniles (Figure 4).

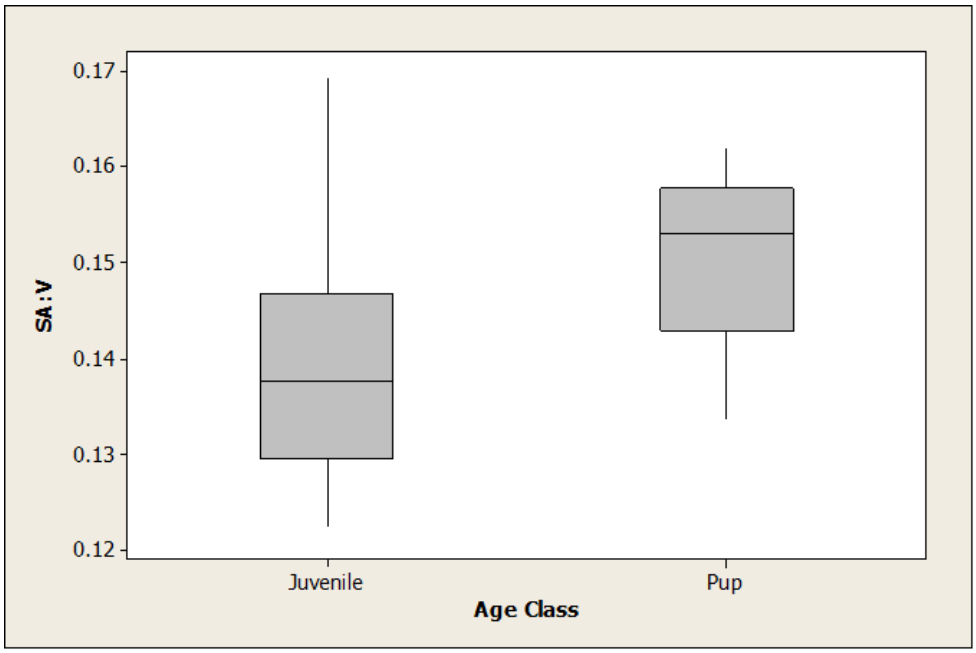

Figure 4. Box and whisker plot of the surface area to volume ratio (SA:V) for juveniles (n=12) and pups (n=10). The horizontal lines within the boxes are group medians, the box limits represent the upper and lower quartiles, and the whisker limits the range of values.

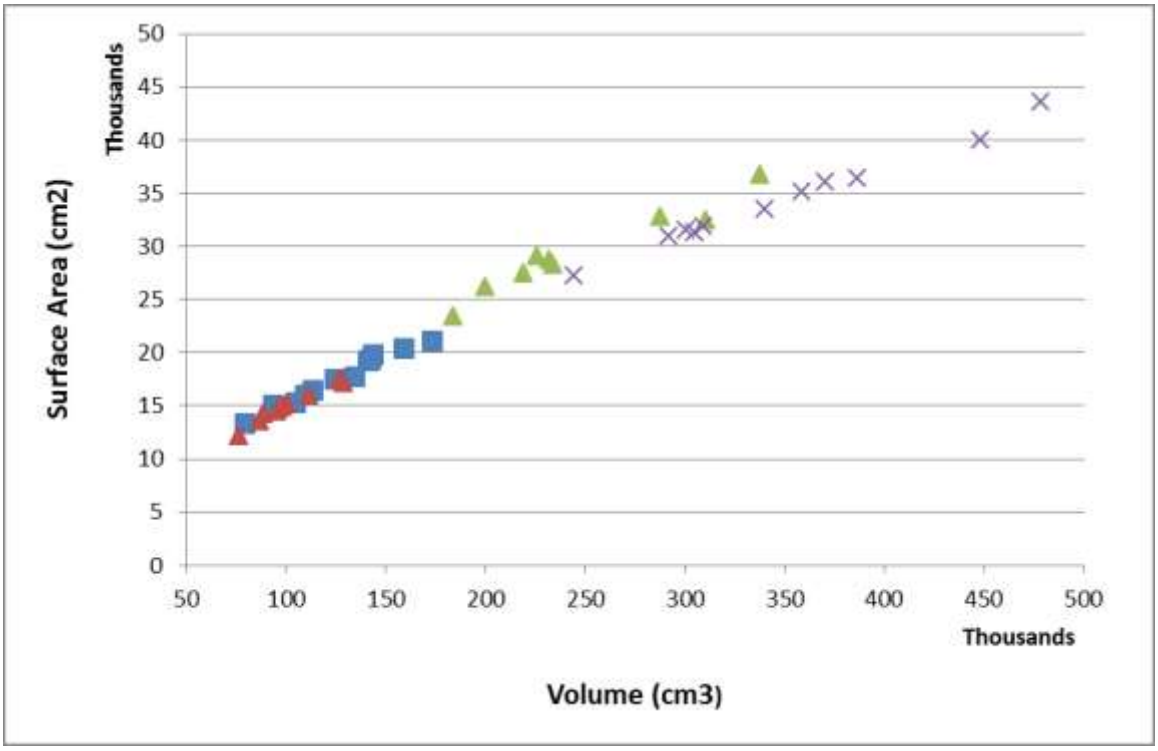

Figure 5. The relationship between surface area to volume ratio (SA:V) and body length for pups (n = 10, red diamonds), juveniles (n = 12, blue squares), non-breeding females (NRFs, n = 11, purple crosses), and post-reproductive females (PRFs, n = 9, green triangles).

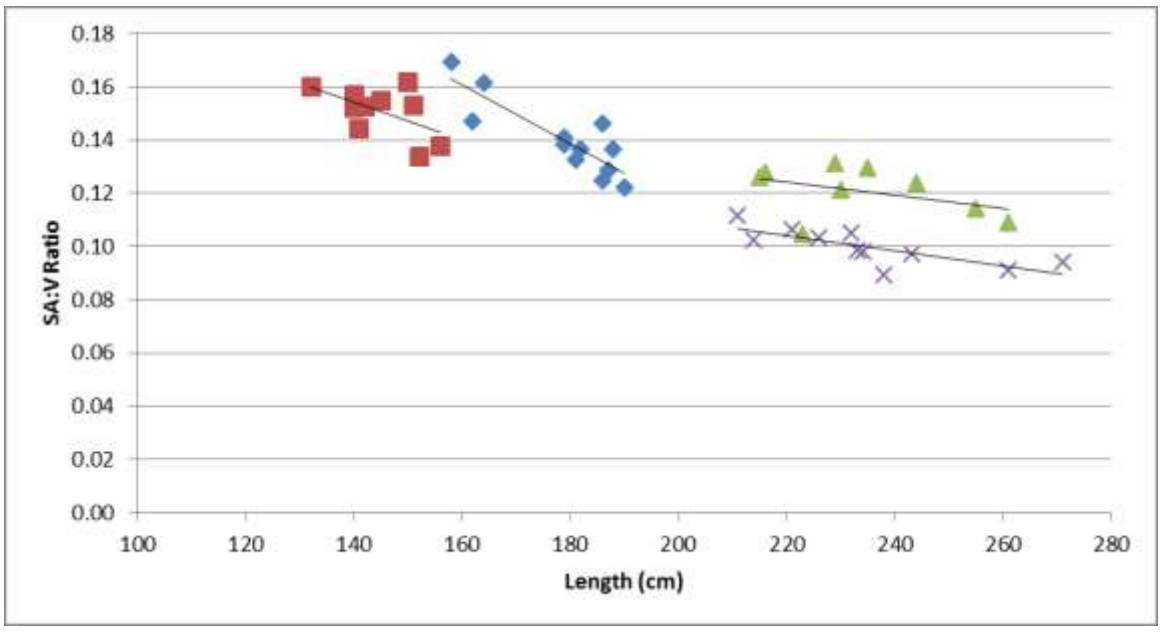

Figure 6. The relationship between surface area to volume ratios (SA:V), and body length for pups (n=10, red squares), juveniles (n=12, blue diamonds), non-breeding females (NRFs, n = 11, purple crosses), and post-reproductive females (PRFs, n = 9, green triangles). Lines are linear regressions for groups.

Projected Growth

All geometric projected growth models (½ sphere, ½ cylinder, bi-conical, and mixed-cone) yielded very similar power relationships for SA:V to body length (Figure 7). We therefore chose to describe the projected growth of juveniles and PRFs through a power equation ($y=ax^b$) directly fitted to the original Photomodeler SA:V data of pups and adult NRFs (n=30). The actual differences between the fitted equation and values derived from adjusted geometric models were smallest for the cone and truncated cone model, but these differences were small (Figure 7).

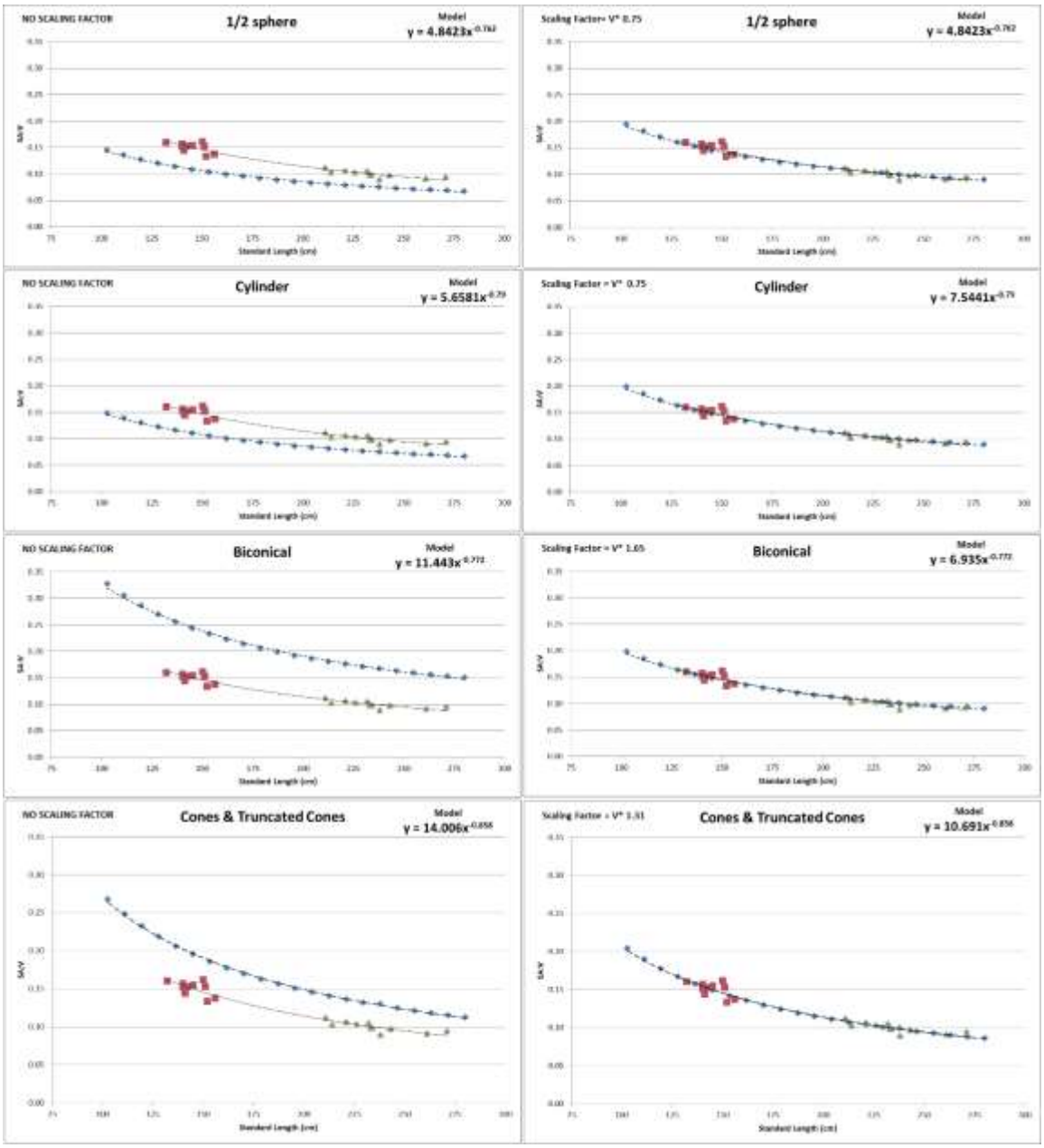

Figure 7. Comparison of four geometric models (half sphere, half cylinder, bi-conical, complete cones and truncated cones – see methods) using actual values for pups (n=10, red squares) and post-reproductive females (PRFs, n=9, blue diamonds). The equation for the curve using actual values is $SA:V = 10.158\ SL^{-0.847}$, while the equations for the models are shown at the top right of each graph, shown without scaling factors (left) and with scaling factors applied to volumes (right). Lines are power regressions for groups.

The equation for this curve is as follows: SA:V = 10.158 $SL^{-0.847}$, where SL is in centimeters, while SA and V are in centimeters squared and cubed respectively. Figure 8 shows SA:V values for juvenile animals in relation to the predicted growth curve. All values for juveniles are higher than predicted growth values. Similarly, values for all but one PRFs are above values for NRFs. Calculated residuals of pup (0.0005 ± 0.008), juvenile (0.014 ± 0.009), NRF (-0.0002 ± 0.004), and PRF (0.021 ± 0.009) data versus the best fit power equation show that juveniles and PRF fall above of predictions with greater SA:V ratios than expected (Figure 9).

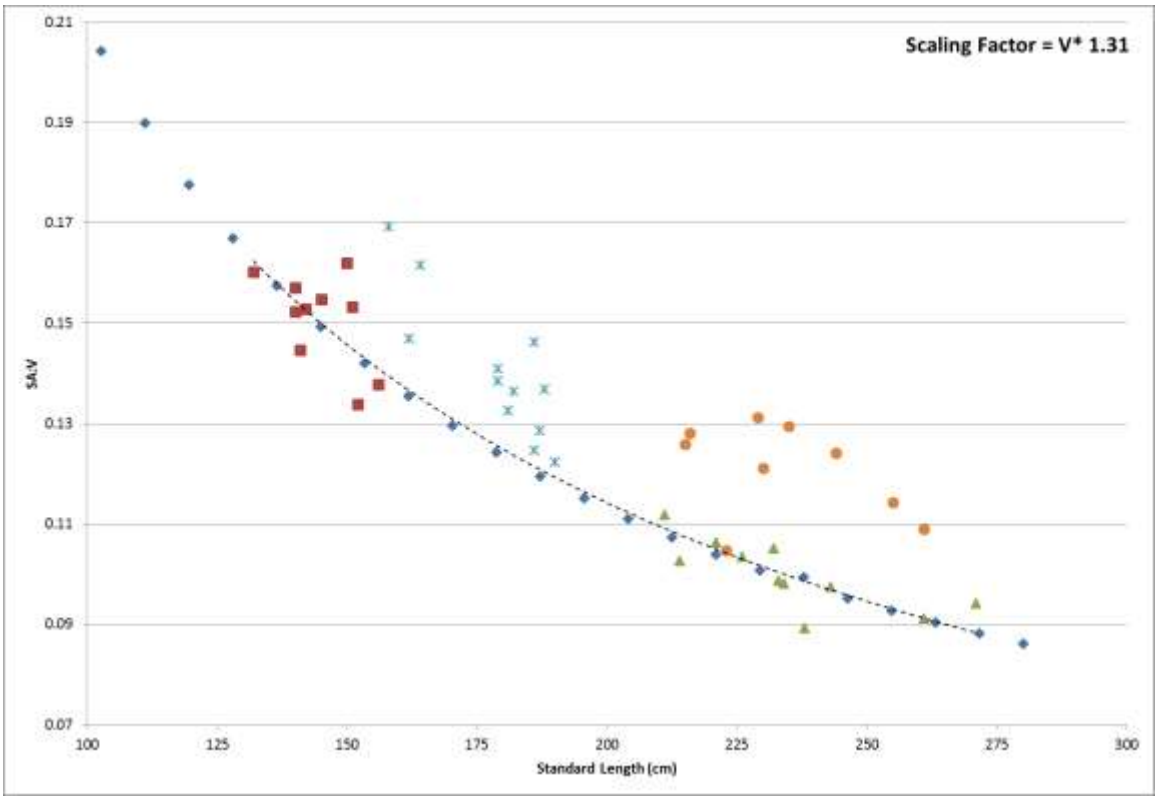

Figure 8. Surface-area-to-volume-ratio (SA:V) values as a function of SL for pups (n = 10, red squares), juveniles (n = 12, blue stars), non-breeding females (NRFs, n = 11, green triangles), and post-reproductive females (PRFs, n = 9, orange circles) (for details see text). The Expected Growth Curve (trend line through blue diamonds) is a power regression through the actual pup and NRF values. The expected values are best described by the equation $y=10.158x^{-0.847}$, $r^2 = 0.95$.

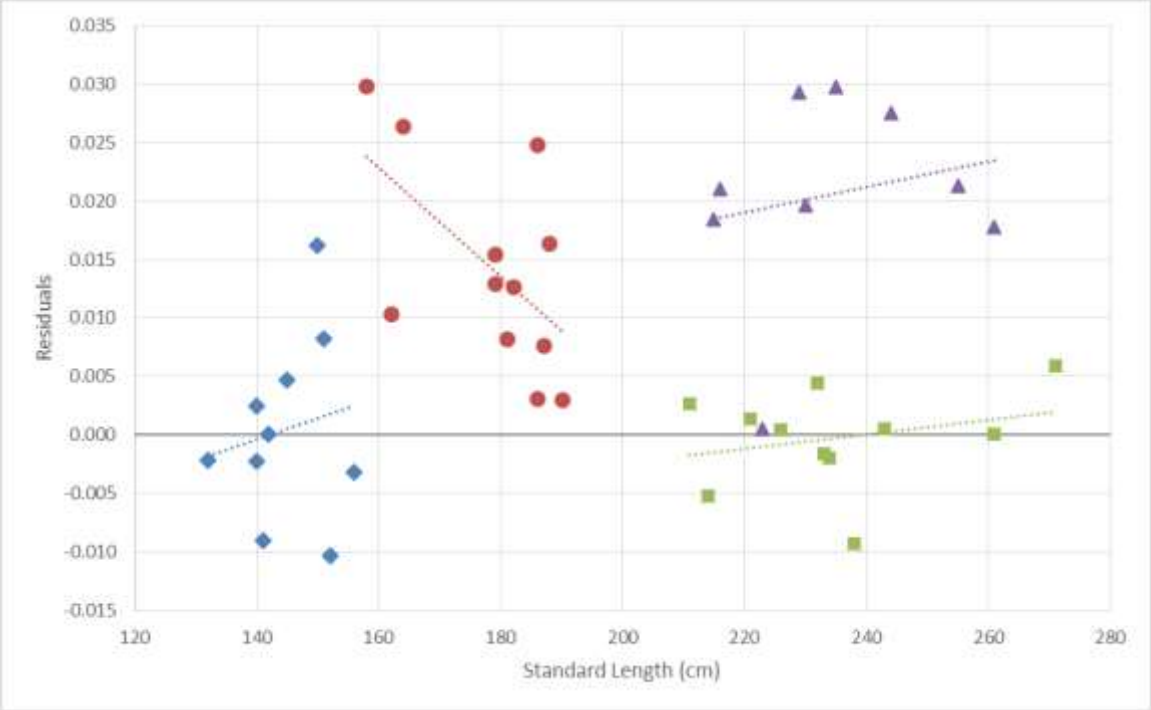

Figure 9. Residuals of actual vs predicted surface-area-to-volume-ratio (SA:V) for a given standard length (SL) for pups (n=10, blue triangles), juveniles (n=12, red circles), non-breeding females (NRFs, n = 11, green squares), and post-reproductive females (PRFs, n = 9, purple triangles).

Mean body density averaged 1.11 ± 0.05 kg/l for pups and 1.15 ± 0.09 kg/l for juveniles, showing no significant difference (P = 0.31, t = 1.03). The average mass of pups was 111.75 ± 16.46 kg, and of juveniles was 148.54 ± 28.49 kg, showing a significant difference in mass between the two age classes (P = 0.001, t = 3.6).

NRFs (371.5 ± 71.2 kg) have a significantly higher body mass than PRFs (270.8 ± 53.4 kg; P = 0.0025, t = -3.51). However, we found no significant difference in mean body density between NRF (1.071 ± 0.057 kg/l) and PRF (1.097 ± 0.043 kg/l; P= 0.26, t = 1.15). The sum of all 10 sampled blubber depth locations (blubber thickness index) were calculated for all NRFs and PRFs (n=21; Table 2). The difference in the blubber

thickness index between PRFs (36.3 ± 9.95 cm cm) and NRFs (55.6 ± 6.40 cm) was significant, with PRF showing much thinner blubber than NRFs ($P < 0.001$, $t = -5.27$; Figure 10). Furthermore, the difference in blubber thickness between pups (46.69 ± 4.38) and juveniles (35.63 ± 9.13) was also significant, with juveniles showing much thinner blubber than pups ($P = 0.002$, $t = 3.99$).

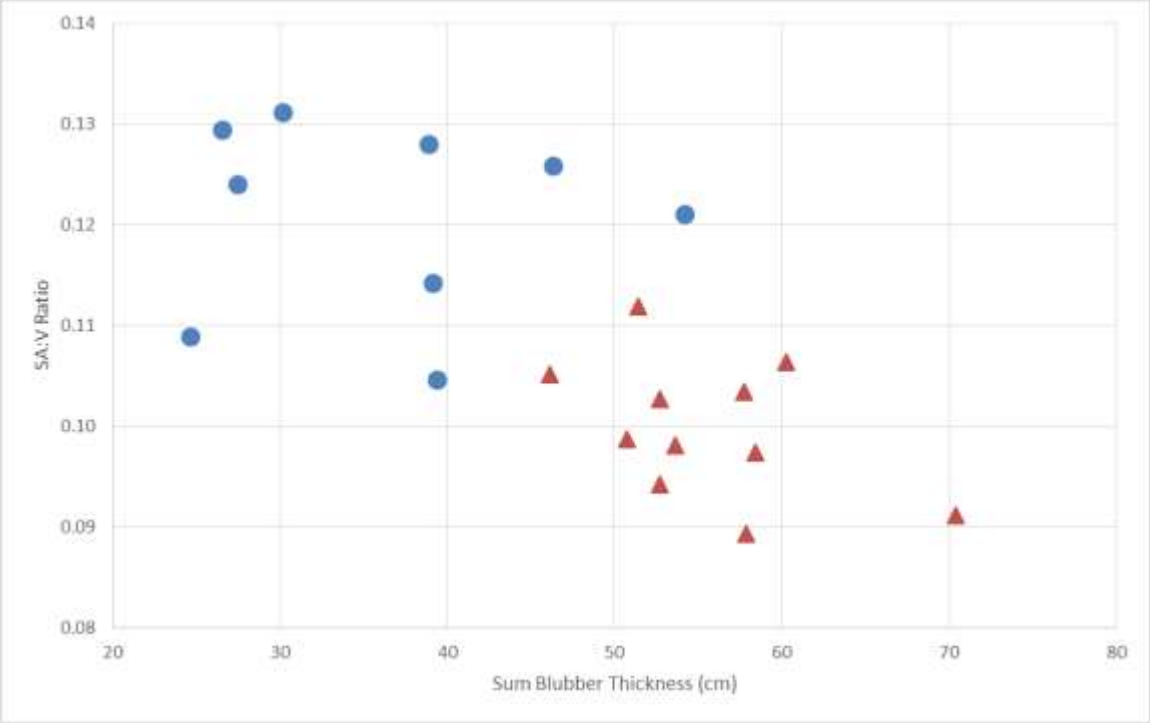

Figure 10. The blubber thickness index for non-breeding females (NRFs, n = 11, red triangles) and post-reproductive females (PRFs, n = 9, blue circles) as a function of the surface-area-to-volume ratio (SA:V).

Table 2. Blubber depths (cm) at all 10 sampled body locations for non-breeding females (NRFs) and post-reproductive females (PRFs), with the blubber thickness index calculated as the sum of all individual blubber depths (n=21)

Animal ID	Class	D1	D2	D3	D4	D5	L1	L2	L3	L4	L5	Sum
LW11-04	NRF	4.0	3.9	3.8	4.1	4.3	4.5	6.3	5.8	4.7	4.9	46.2
LW12-53	NRF	3.98	4.81	5.35	4.73	5.08	3.78	5.67	6.39	5.66	5.99	51.4
LW12-54	NRF	4.11	5.64	5.92	5.54	5.58	4.57	8.64	6.77	6.05	5.58	58.4
LW11-03	NRF	5.8	5.3	5.4	4.8	5.6	5.5	8.1	7.7	6.2	5.8	60.2
LW12-55	NRF	4.60	4.62	5.42	5.26	5.95	-	7.73	7.36	5.90	5.86	52.7
LW12-52	NRF	3.87	5.16	5.92	5.26	5.36	4.81	6.64	7.64	6.67	6.42	57.8
LW12-56	NRF	4.10	4.54	4.67	4.54	4.82	3.82	7.11	5.80	5.55	5.80	50.8
LW12-58	NRF	5.34	5.29	6.30	5.77	5.85	5.11	6.05	6.12	5.74	6.30	57.9
LW12-60	NRF	3.70	4.30	5.29	5.33	4.89	3.32	6.99	7.21	5.58	6.08	52.7
LW12-57	NRF	4.97	5.91	6.52	6.69	7.01	4.68	8.46	8.74	8.77	8.66	70.4
LW12-59	NRF	4.70	5.13	5.80	5.14	5.26	4.77	5.67	5.24	5.80	6.11	53.6
LW11-14	PRF	4.5	2.8	3.7	3.8	3.2	4.5	5.4	3.9	3.5	3.5	38.9
LW12-20	PRF	2.30	2.43	-	2.81	2.68	2.44	3.65	2.77	2.61	2.97	24.7
LW12-14	PRF	4.09	2.92	3.98	4.00	3.78	4.38	4.09	4.36	4.02	3.76	39.4
LW12-17	PRF	2.56	1.97	2.61	2.81	3.05	2.81	2.52	2.67	3.32	3.12	27.4
LW12-13	PRF	2.70	2.81	2.46	2.76	2.81	4.27	4.18	2.63	2.70	2.85	30.2
LW12-19	PRF	2.34	2.54	2.81	2.56	2.32	2.87	3.52	2.68	2.48	2.41	26.5
LW12-18	PRF	3.31	2.78	3.66	3.80	3.90	5.02	5.95	3.42	3.50	3.77	39.1
LW12-07	PRF	5.29	4.14	5.02	5.51	5.58	5.77	6.17	5.45	5.72	5.53	54.2
LW12-04	PRF	3.82	4.22	4.74	4.20	4.55	4.46	6.11	4.89	4.57	4.79	46.4

DISCUSSION

The classic notion that 'larger is better' in a thermally challenging environment is primarily driven by declining SA:V ratios with increasing size, all else being equal (Blix and Steen 1979; Noren et al. 2008). However, it has been noted that Weddell seal pups are more rotund than juveniles, who appear thinner, stretched, and leaner; thus possibly leading to an increased SA:V ratio for a given mass. This led us to test the classic notion of an ontogenetically declining SA:V ratio in our study of 42 Weddell seals from McMurdo Sound, Antarctica.

Contrary to our initial expectations, juveniles on average *do* have a significantly smaller SA:V ratio than pups (Figure 4). Therefore, the effect of the "thinning" of the body shape in the transition from pup to juvenile does not outweigh the overall effect of increasing body length on the SA:V ratio. Within both groups, the SA:V ratio declined with increasing body length, however the smallest juveniles had a larger SA:V ratio than the largest pups (Figure 6). Furthermore, for the juveniles and pups whose lengths are comparable, SA:V ratios are higher within the juvenile age class (Figure 6). Thus suggesting that the SA:V ratio of juveniles is influenced by both increasing length and morphological changes. Thus, there may be a thermoregulatory challenge associated with the transition to independence and concomitant change in the body shape of young Weddell seals.

Expected Growth Curve Model

We looked at how Weddell seals grow from pups to NRFs by modeling proportional growth between these two age classes and body shapes. We used a geometric model using complete and truncated cones (Figure 3), to determine that proportional growth follows a power equation. From a power equation fit to pup and adult NRF data, we derived a prediction for SA:V ratios for a given body length (Figure 8). A comparison of actual SA:V ratios for juveniles to these predicted values revealed juveniles to uniformly exhibit SA:V ratios greater than the predicted estimates (Figure 8, 9). This does indeed suggest that the morphological transition from rotund pup to thinner juvenile, contributes to the SA:V ratios observed in juveniles.

PRFs are another interesting case study, in that they are challenged by their significant weight (and energy) loss during lactation. Since it is unlikely that the skin and therefore SA shrinks much during lactation, one would expect their SA:V values to be consistently above the predicted power fit for NRFs, which indeed was the case (Figure 9). Thus, PRFs as a demonstrably 'challenged' control group also exceed the SA:V ratios predicted by the power fit shown in Figure 8. Blubber thickness measurements indicated that PRFs had significantly less blubber than NRFs, suggesting that the energetic demands of lactation and meeting basic maintenance needs might be covered through fat metabolism. With pinniped lean tissue density at approximately 1.07 g/cm^3, and blubber at approximately 0.9 g/cm^3 (Nordoy and Blix 1985), the body density of fat-burning PRFs should be higher than that of NRFs (mean body density 1.07 g/cm^3). However, there was no significant difference in body density between these groups. PRFs thus lost

a significant amount of mass, whilst retaining the same density as NRFs. This in turn suggests that lactating females may be catabolizing protein in addition to burning fat, during the lactational fasting period.

There is no consistent definition of the frequently used term ‘body condition’. Well-fed animals in good nutritional state with ample energy reserves in the form of adipose tissue are often described as being in good condition (Gales et al. 1994; Jonker and Trites 2000; Biuw et al. 2003). A common practical use in contemporary studies is the ratio of adipose to lean tissue, suggesting that the more fat you have, the better your body condition (Falke et al. 1985; Noren et al. 2008).

However, for our PRFs that as capital breeders very likely utilized a substantial portion of their energy stores, we found no evidence of a shift in the adipose to lean tissue ratio via altered density. This leads us to conclude that density or the ratio of adipose to lean tissue is a poor proxy of body condition. Alternatively, we propose that the SA:V value in relation to a ratio predicted for a given body length might be a better indicator of body condition/state, possibly in combination with a cumulative blubber thickness measure. Similarly, the mean body density did not differ between pups and juveniles even while juveniles had a lower blubber thickness index than pups. As with the comparison between the PRFs and NRFs, the blubber index and SA:V vs predicted values comparisons suggest that juveniles represent a challenged life history stage in Weddell seals.

When considering both the blubber thickness index and the SA:V ratio in relation to values predicted for a given length, our study suggests both juveniles and PRFs to be

likely energetically challenged through the twin effects of reduced insulation and disadvantageous SA:V ratios. This morphometric set of measurements may yield a better assessment of body condition for pinnipeds than the ratio of adipose to lean tissue, or a direct comparison of SA:V ratios alone.

REFERENCES

Baker WH (1960) Elements of photogrammetry. Ronald Press

Berta A, Sumich JL, Kovacs KM (2005) Marine mammals: evolutionary biology. Academic Press

Biuw M, McConnell B, Bradshaw CJ, et al. (2003) Blubber and buoyancy: monitoring the body condition of free-ranging seals using simple dive characteristics. J Exp Biol 206:3405–3423.

Blix AS, Steen JB (1979) Temperature regulation in newborn polar homeotherms. Physiol Rev 59:285–304.

Bryden MM (1972) Growth and development of marine mammals. Funct Anat Mar Mamm 1:1–79.

Burns JM (1999) The development of diving behavior in juvenile Weddell seals: pushing physiological limits in order to survive. Can J Zool 77:737–747.

Burns JM, Testa JW (1997) Developmental changes and diurnal and seasonal influences on the diving behaviour of Weddell seal (Leptonychotes weddellii) pups. Antarct Communities Species Struct Surviv Ed B Battagl J Valencia Walt Camb Univ Press Camb 328–334.

Dearborn JH (1965) Food of Weddell seals at McMurdo sound, Antarctica. J Mammal 37–43.

Elsner R, Hammond DD, Denison DM, Wyburn R (1977) Temperature regulation in the newborn Weddell seal Leptonychotes weddellii. Adapt Antarct Ecosyst GA Llano Ed Smithson Inst Wash DC 531–540.

Falke KJ, Hill RD, Qvist J, et al. (1985) Seal lungs collapse during free diving: evidence from arterial nitrogen tensions. Science 229:556–558.

Gales R, Renouf D, Noseworthy E (1994) Body-Composition of Harp Seals. Can J Zool-Rev Can Zool 72:545–551. doi: 10.1139/z94-073

Hadley GL, Rotella JJ, Garrott RA, Nichols JD (2006) Variation in probability of first reproduction of Weddell seals. J Anim Ecol 75:1058–1070. doi: 10.1111/j.1365-2656.2006.01118.x

Hansen S, Lavigne DM (1997) Ontogeny of the thermal limits in the harbor seal (Phoca vitulina). Physiol Zool 70:85–92.

Hokkanen J (1990) Temperature Regulation of Marine Mammals. J Theor Biol 145:465–485. doi: 10.1016/S0022-5193(05)80482-5

Innes S, Worthy G, Lavigne D, Ronald K (1990) Surface-Areas of Phocid Seals. Can J Zool-Rev Can Zool 68:2531–2538. doi: 10.1139/z90-354

Irving L (1973) Aquatic Mammals. Comp. Physiol. Thermoregul. Academic Press, New York, pp 47–96

Iversen JA, Krog J (1973) Heat production and body surface area in seals and sea otters. Nor J Zool 21:51–54.

Jonker R a. H, Trites AW (2000) The reliability of skinfold-calipers for measuring blubber thickness of Steller sea lion pups (Eumetopias jubatus). Mar Mammal Sci 16:757–766. doi: 10.1111/j.1748-7692.2000.tb00970.x

Kaufman GW, Siniff DB, Reichle R (1975) Colony behavior of weddell seals, Leptonychotes weddelli, at Hutton Cliffs, Antarctica. Rapp. Proces-Verbaux Reun. Den.

Kooyman GL (1968) An analysis of some behavioral and physiological characteristics related to diving in the Weddell seal. Wiley Online Library

Kooyman GL, Kooyman GL (1981) Weddell seal, consummate diver. Cambridge University Press New York

Learmonth JA, MacLeod CD, Santos MB, et al. (2006) Potential effects of climate change on marine mammals. Oceanogr Mar Biol 44:431.

Mellish J-AE, Hindle AG, Horning M (2011) Health and condition in the adult Weddell seal of McMurdo Sound, Antarctica. Zoology 114:177–183.

Mellish J-AE, Horning M, York AE (2007) Seasonal and spatial blubber depth changes in captive harbor seals (Phoca vitulina) and Steller's sea lions (Eumetopias jubatus). J Mammal 88:408–414.

Mellish J-AE, Tuomi PA, Hindle AG, Horning M (2010) Chemical immobilization of Weddell seals (*Leptonychotes weddellii*) by ketamine/midazolam combination. Vet Anaesth Analg 37:123–131. doi: 10.1111/j.1467-2995.2009.00517.x

Mellish J-AE, Tuomi PA, Horning M (2004) Assessment of ultrasound imaging as a noninvasive measure of blubber thickness in pinnipeds. J Zoo Wildl Med 35:116–118.

Nadel ER (1984) Energy exchanges in water. Undersea Biomed Res 11:149–158.

Nordoy E, Blix A (1985) Energy-Sources in Fasting Grey Seal Pups Evaluated with Computed-Tomography. Am J Physiol 249:R471–R476.

Noren SR, Pearson LE, Davis J, et al. (2008) Different Thermoregulatory Strategies in Nearly Weaned Pup, Yearling, and Adult Weddell Seals (*Leptonychotes weddelli*). Physiol Biochem Zool 81:868–879. doi: 10.1086/588489

Ridgway SH (1972) Homeostasis in the aquatic environment. Mamm Sea Biol Med 590–747.

Roscow EVH (2001) Thermoregulation in Steller sea lions: a modelling approach. Texas A & M University

Schmidt-Nielsen K (1984) Scaling: why is animal size so important? Cambridge University Press

Stauffer GE, Rotella JJ, Garrott RA (2013) Birth-year and current-year influences on survival and recruitment rates of female Weddell seals. Popul Ecol 55:405–415. doi: 10.1007/s10144-013-0379-0

Waite JN, Schrader WJ, Mellish J-AE, Horning M (2007) Three-dimensional photogrammetry as a tool for estimating morphometrics and body mass of Steller sea lions (Eumetopias jubatus). Can J Fish Aquat Sci 64:296–303.

Watts P, Hansen S, Lavigne D (1993) Models of Heat-Loss by Marine Mammals - Thermoregulation Below the Zone. J Theor Biol 163:505–525. doi: 10.1006/jtbi.1993.1135